Extraordinary improvement in scintillation detectors via post-processing with ASEDRA—solution to a 50-year-old problem

E. LaVigne, G. Sjoden*, J. Baciak, and R. Detwiler
FINDS, University of Florida/NRE, 202 NSB, Gainesville, FL 32611-8300 USA

ABSTRACT

We have developed a ground-breaking algorithm, ASEDRA, to post-process scintillator detector spectra to render photopeaks with high accuracy. The post-processed spectrum is comparable with resolved full energy peaks rendered by high resolution HPGe semiconductor detectors. ASEDRA, or "Advanced Synthetically Enhanced Detector Resolution Algorithm," is currently applied to NaI(Tl) detectors, which are robust, but suffer from poor energy resolution. ASEDRA rapidly post-processes a NaI(Tl) detector spectrum over a few seconds on a standard laptop without prior knowledge of sources or spectrum features. ASEDRA incorporates a novel denoising algorithm based on an adaptive Chi-square methodology called ACHIP, or "Adaptive Chi-quare Processed denoising." Application of ACHIP is necessary to remove stochastic noise, yet preserve fine detail, and can be used as an independent tool for general noise reduction. Following noise removal, ASEDRA sequentially employs an adaptive detector response algorithm to remove the spectrum attributed to specific gammas. Tests conducted using a 2"x2" NaI(Tl) detector, along with a HPGe detector demonstrate the accuracy of ASEDRA; in this paper, we present results using a ^{152}Eu source. Analysis of ASEDRA results show correct identification of at least 15 photopeaks from ^{152}Eu, with relative yield ratios of major lines to better than a factor of two for most cases (referencing the ^{152}Eu 344 keV photopeak), enabling better than a factor of four improvement in resolving peaks compared with unprocessed NaI(Tl). Moreover, denoising and synthetic resolution enhancement algorithms can be adapted to any detector. ACHIP and ASEDRA are covered under a Provisional Patent, Registration Number #60/971,770, 9/12/2007, USPTO.

Keywords: ASEDRA, Algorithm, Synthetic Enhancement, Sodium-Iodide, Post processing

1. INTRODUCTION

Radiation detectors are used every day in numerous applications, including medical imaging, oil well logging, and in environmental health and safety inspections. Because they are relatively inexpensive and easy to operate at room temperature, scintillation radiation detectors have seen wide use--the highest visibility application of these detectors in recent years has been inspection of cargo as it enters the United States via border crossings, monitored by the Department of Homeland Security Customs and Border Protection Service [1]. Due to the potential threat from nuclear terrorism, the detection of rogue nuclear materials, before they enter the US, is absolutely essential. Scintillation radiation detectors, including inorganic crystals such as sodium-iodide [2], have proven quite useful, but for the past 50 years, they have been limited by poor spectral resolution; often, more expensive, less portable detectors (such as High Purity Germanium (HPGe)) must be used to provide a positive confirmation of the presence of nuclear materials, particularly for Naturally Occurring Radioactive Materials (NORM). NORM is present in numerous shipments, in medical isotope shipments, or even in cat litter. Discerning NORM in routine shipments apart from Special Nuclear Materials that may be present in a weapon is a challenge to avoid false positives or negatives, and low resolution detectors, un-assisted, may not be up to the task. For this reason, extensive research efforts have been focused on improving room temperature detector resolution using different detector materials since the invention of sodium iodide detectors [3]. To address this issue, in addition to research on new materials, we have also focused on algorithms to improve the quality of the radiation signatures derived from reliable scintillator detectors like sodium iodide. Hence, we have developed a ground-breaking algorithm, ASEDRA ("Advanced Synthetically Enhanced Detector Resolution Algorithm"), to post-process scintillator detector spectra to render photopeaks with high accuracy.

*sjoden@ufl.edu

Chemical, Biological, Radiological, Nuclear, and Explosives (CBRNE) Sensing IX,
edited by Augustus Way Fountain III, Patrick J. Gardner, Proc. of SPIE Vol. 6954,
695416, (2008) · 0277-786X/08/$18 · doi: 10.1117/12.777295

In the past decade, a number of researchers have performed algorithm research to improve poorly resolved spectra from room temperature scintillators, and with some success [4,5,6]. The ASEDRA algorithm we have developed yields a significant leap forward in post-processing algorithms [7, 8]. Our approach is straight forward, but leads to accurate results—we apply a post-processing algorithm to attribute complete spectrum data from individual photopeaks separately from the integrated radiation spectrum output from a detector in a manner to render highly accurate signatures (resolved photopeaks), which can then be aliased to nuclides of interest for positive identification using a nuclide identification tool. The results rendered from an ASEDRA post-processed spectrum have proven to be very comparable with well resolved spectra from more expensive, nitrogen cooled HPGe semiconductor detectors. In this paper, we present the mechanics of the ASEDRA algorithm, followed by examples of its application to real radiation spectra using sodium iodide detectors, along with HPGe detector spectra (collected side by side) for unequivocal comparison. This is followed by a discussion, conclusions, and future work.

2. THE ASEDRA ALGORITHM

In this section, we describe the components and mechanics of the ASEDRA algorithm. A very first and critical step in processing a collected gamma spectrum begins with a robust noise removal process. This is extremely important since for short count/few-count spectra, noise removal without further degrading spectral resolution, is essential. After significant research to perform optimum stochastic component removal with preservation of spectral resolution, the ACHIP tool was developed and subsequently integrated into ASEDRA. Following noise removal, an energy sweeping and attribution process using high resolution Detector Response Functions, generated using Monte Carlo simulation, are applied to achieve extraction and attribution of photopeaks in the spectrum under consideration. Detailed descriptions of these processes are provided below.

2.1 Stochastic Noise Removal with ACHIP

Traditional noise smoothing processes, such as *weighted averaging*, do indeed yield smoothing, but lead directly to a loss in resolution. A more robust procedure based on a Chi-square analysis can be used to determine whether a difference between counts in neighboring channels, assumed to have similar uncertainties, is statistically significant, or if it is noise. The criteria of whether or not the data is "noise" would then depend on (i) a user-specified test parameter "alpha" (significance value) spanning from [0.005, 0.995], (ii) the number of degrees of freedom (collective points considered), and (iii) the associated confidence interval assigned to the "alpha" value for the data. The Chi-square metric computed for actual values n_i vs. "expected" modeled values $E(n_i)$ in adjacent channels is

$$X^2 = \sum_i \frac{(n_i - E(n_i))^2}{E(n_i)} \tag{1}$$

Our ACHIP tool uses a Chi-square basis with a user-specified alpha value for stochastic noise removal at each datapoint in a spectrum using parabolic fits, and smaller "alpha" values lead to more smoothing (noise removal). The process is very efficient, since it is implemented using a Gram-Schmidt construct. Parabolic fit models in the form of $f(x) = c_0 + c_1x + c_2x^2$ also may be defined by a set of vectors $(\boldsymbol{v_0, v_1, v_2})$ to represent $(\boldsymbol{1, x, x^2})$, and form a parabola vector of the form $\boldsymbol{u = c_0v_0 + c_1v_1 + c_2v_2}$. Constants (c_i) are derived so that the parabola vector ($\boldsymbol{u}$) and the actual measured data values ($\boldsymbol{m}$) are as close as possible in value, therefore minimizing the differences between both. ACHIP computes the value of the parabola vector by first expressing it as a linear combination of orthonormal vectors $(\boldsymbol{w_0, w_1, w_2})$. ACHIP then employs Gram-Schmidt orthogonalization to select the set of orthonormal vectors that will be equivalent to map all linear combinations of the set of vectors, $(\boldsymbol{v_0, v_1, v_2})$. The orthonormal set of vectors used depends on the number of channels considered in the data set, and after being computed, these are stored for re-use when considering the same datapoint size in subsequent applications (saving computational time). With a given set of orthonormal vectors over n datapoints, noise reduction is implemented.

By starting with three channels, including the "targeted" channel of interest (centered) where noise is to be removed, the parabolic model is initially fit to match the original three points via a least squares fit. Additional surrounding points are

considered, keeping the data point of interest in the center, where new parabolic fits for all points are determined. When the parabolic model, for the number of points considered, no longer satisfies the user-specified Chi-square test metric, the model that *just previously* satisfied the Chi-Square criteria, using (*n*-1 points fit), where the Chi-square test *was* satisfied is used. This ensures that an "elevation" in the spectrum is a "true feature", and readily eliminates artifacts that are a result of stochastic sampling; the other unique advantage of this process is that no artifacts are introduced by the process to degrade resolution, which is a very important factor for subsequent applications with ASEDRA. Of course, the "alpha" parameter must be appropriate for the data; however, we typically will apply a "maximum" denoising by setting an alpha value of 0.005. The fitting of the parabolic models is continued for all channels of the data set and the background spectrum to determine the appropriate denoised value for each channel. In any event, ACHIP has been streamlined to execute on the order of a few hundred milliseconds for a typical spectrum, which is ideal for post processing applications. Due to the remarkable results achieved, ACHIP has been broken out of ASEDRA as a stand-alone tool with a GUI and, like ASEDRA, is also patented.

2.2 ACHIP Results

The results of the ACHIP noise reduction procedure described in Section 2.1 are achieved rapidly with dramatic results. The plot on the left (Figure 2.2.1) is a Monte Carlo pulse height tally generated using 1.2E7 histories from a 350 keV gamma ray; the plot on the right (Figure 2.2.2) is the same tally with noise removal by ACHIP, accomplished in <1 s on a one-CPU laptop PC with an alpha of 0.005. Note that resolution is preserved in all true data. It is of note that ACHIP has also been established as a 2-dimensional denoising tool for image processing to reduce stochastic interference in images without a loss of resolution; testing of this is ongoing.

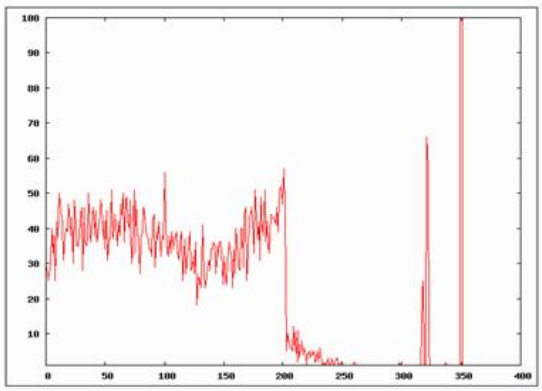

Detector Spectrum before denoising

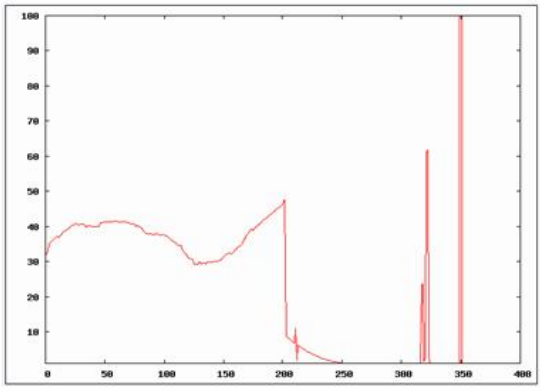

Detector Spectrum after denoising

Figure 2.2.1 (Left) and Figure 2.2.2 (Right). Examples of ACHIP denoising software (before, Figure 2.2.1, and after, in Figure 2.2.2) applied to a Monte Carlo simulation pulse height tally. The simulation was performed using MCNP5.

Note the fine detail, including the X-ray escape peaks, are preserved, and stochastic artifacts are nearly all removed. The remaining artifact at ~210 keV in Figure 2.2.2 is not real, yet was not removed by ACHIP. We have found that when too few counts are present (e.g., < 10, where Poisson statistics fall apart), noise reduction benefits are limited and may fail.

2.3 ASEDRA Energy Sweep

The ASEDRA algorithm is straight forward in principle—following spectrum and background noise removal with ACHIP, further processing can be associated with a conventional "strip" procedure [5], although in ASEDRA the *entire spectrum* attributed to each identified photopeak is sequentially removed from the integral detector spectrum using Monte Carlo generated Detector Response Functions (DRFs) for a sodium iodide detector. DRFs were generated based on typical source-detector configurations for (i) an unshielded source and (ii) a shielded source using a 1 cm thick iron

shield, determined from detector pulse height tallies to simulate true detector response without the broadening of electronics. Broadening of the finely resolved DRFs to alias responses in a real scintillation detector system must then be performed. This is accomplished by applying a Gaussian function with a low energy tailing correction that is detector and energy dependent. Therefore, this is based on a simple energy dependent Full-Width-at-Half -Maximum (FWHM) table, along with an energy calibration (ECAL) file spanning the energies of interest supplied by the user, and are treated by ASEDRA as piecewise linear functions. We note that both the FWHM and ECAL data files are detector related details required for any standard radiation spectrometer, and besides the sample spectrum and the background spectrum, are the only outside data requirements necessary to execute ASEDRA. Peak search begins at the high-energy end of the net spectrum, and locating one photopeak at a time, the entire detector response for each photopeak is recursively subtracted, as determined by DRFs defined for a described geometry, continuing this process until no further photopeaks can be identified. Essentially, ASEDRA is a rapid post-processing algorithm that synthetically renders photopeaks from a collected spectrum using a robust, physics-based approach.

A flow diagram in Figure 2.3.1 shows how ASEDRA processes a spectrum.

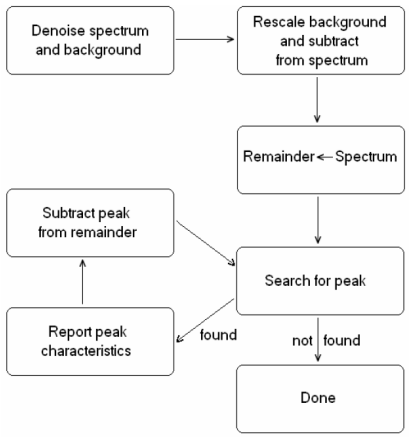

Figure 2.3.1 ASEDRA Processing flow

Once a sample spectrum is collected, all information required for post processing is described in a file called "*process.txt*", where an example is included in Figure 2.3.2. Options for low energy tailing, denoising, DRF shielding, minimum peak amplitude rejection thresholds, and scattered counts scaling (discussed later) are user selectable.

process.txt - Notepad

File Edit Format View Help

```
Sample File
"C:\ASEDRA\ASEDRAscL\blueprint2rev\NaIPuBe10min.Spe"
Background File
"C:\ASEDRA\ASEDRAscL\blueprint2rev\NaIBKG0.Spe"
Background Significance Factor (1 for correct background subtraction)
1
Max Energy FWHM callibration table: file in "position(keV) width(keV)" format
"C:\ASEDRA\ASEDRAscL\blueprint2rev\FWHM.txt"
Low energy tailing: height ratio, FWHM(keV)
0 1
Energy Callibration Table
"C:\ASEDRA\ASEDRAscL\blueprint2rev\Energy.txt"
Chi-squared threshold (negative value turns on adaptive chi filter)
-1
Alpha for adaptive chi (max smoothing is 0.005, min smoothing is 0.1, recommended 0.05)
0.01
Shielding Material (0=air,1=iron)
1
Rejection Threshold (minimum peak height)
10
Relative channel threshold (peak must represent a significant percent of the total spectrum in a channel)
5
Scattered counts scale factor to account for unknown geometry
1
```

Figure 2.3.2 ASEDRA process.txt settings file

The sample and background spectrum file are presumed to be in the Ortec MAESTRO data spectrum format. An excerpt from a MAESTRO spectral data file is shown below in Fig 2.3.3. In particular, notice that there are 12 lines at the beginning of the file before the count data starts, that the first number on the 10th line indicates detector live time, and that the 12th line indicates the channel indices for the first and last channels.

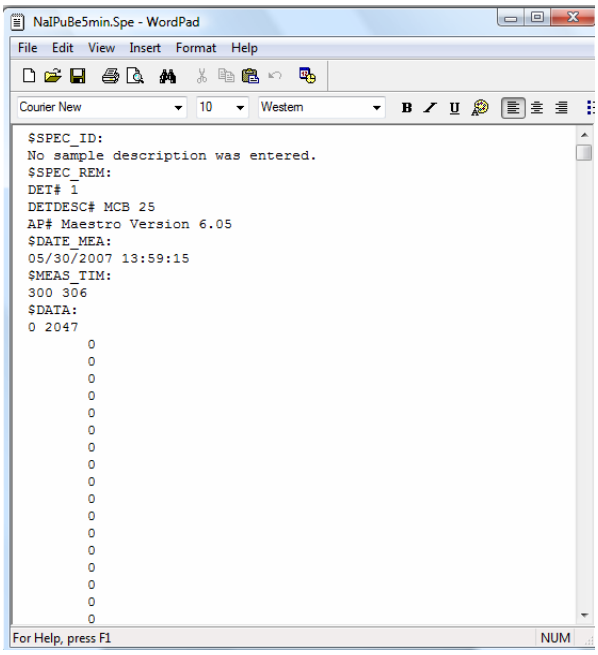

Figure 2.3.3 MAESTRO sample header file format

For ASEDRA to properly identify photopeaks in a convoluted spectrum, it is important to have accurate energy and resolution calibration values for the detector system provided by the user as text files (with consistent names as noted in the *process.txt* input). Resolution must be given as FWHM values in keV. Again, correct peak extraction relies on the fact that these files are established to span as much of the "energy-count" phase space as is practical. This is essential to enable ASEDRA to properly deconvolve photopeak data. Examples of these calibration files are shown in Figure 2.3.4. Note that no other a-priori information is necessary for ASEDRA.

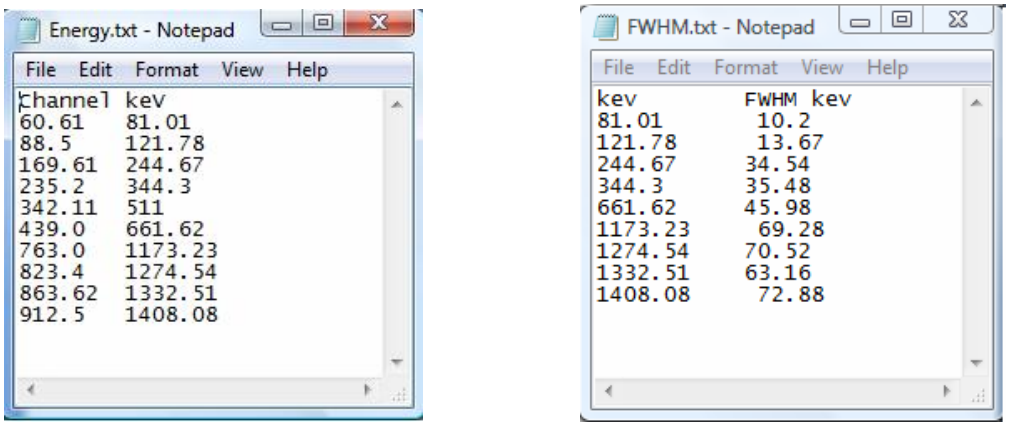

Figure 2.3.4 ECAL energy (left) and FWHM resolution (right) calibration files

2.4 ASEDRA GUI

A Graphical User Interface written in Java has been developed to enable a visual application of the Algorithm to spectrum files. A screen shot of the GUI is available in Fig 2.4.1.

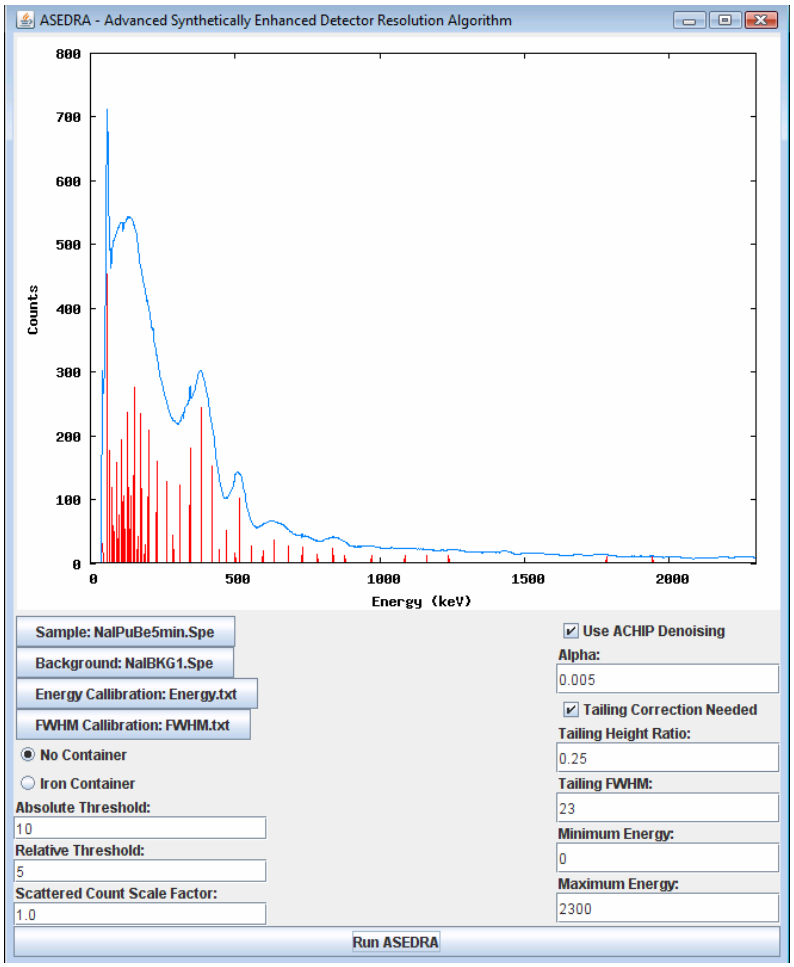

Figure 2.4.1. Screen Shot of Java ASEDRA GUI, showing a 5 min WGPu spectrum and associated peaks extracted

2.4 Adaptability of DRFs

As discussed previously, ASEDRA relies on Detector Response Functions (DRFs) pre-computed using Monte Carlo simulations for a defined source-detector geometry. Therefore, the DRF geometry is intended to be approximately consistent with the actual geometry being applied. If this is not the case, and the detector geometry is substantially different from that used in original DRFs, there are two options that can be considered. One is to recompute DRFs for the new geometry, which can require substantial effort, but is effective. Another approach that has proven to be both straight forward and effective requires a detector calibration using one or more check sources using the new geometry; in most cases, increased Compton, geometry, and other effects can be properly accounted for with existing DRFs by using an available "scattered counts scale factor," or SCSF in the ASEDRA algorithm. While it is best to have DRFs tuned to a particular geometry, the SCSF reduces algorithm performance sensitivities to the specific pre-computed DRF geometries. Therefore, use of the SCSF enables one to adapt generic DRFs to a specific application, enabling ASEDRA to be a flexible post processor for many applications using default DRFs.

3. TEST RESULTS

3.1 Eu-152 NaI and HPGe Results

Side by side tests of a 2"x2" NaI(Tl) detector spectrum post-processed by ASEDRA compared directly with a germanium detector (with the same geometry) have demonstrated the ASEDRA methodology is highly accurate. In addition to tests with more simple spectra, the spectrum from a ^{152}Eu source counted for 300 s with NaI(Tl) is presented in Figure 3.1.1.

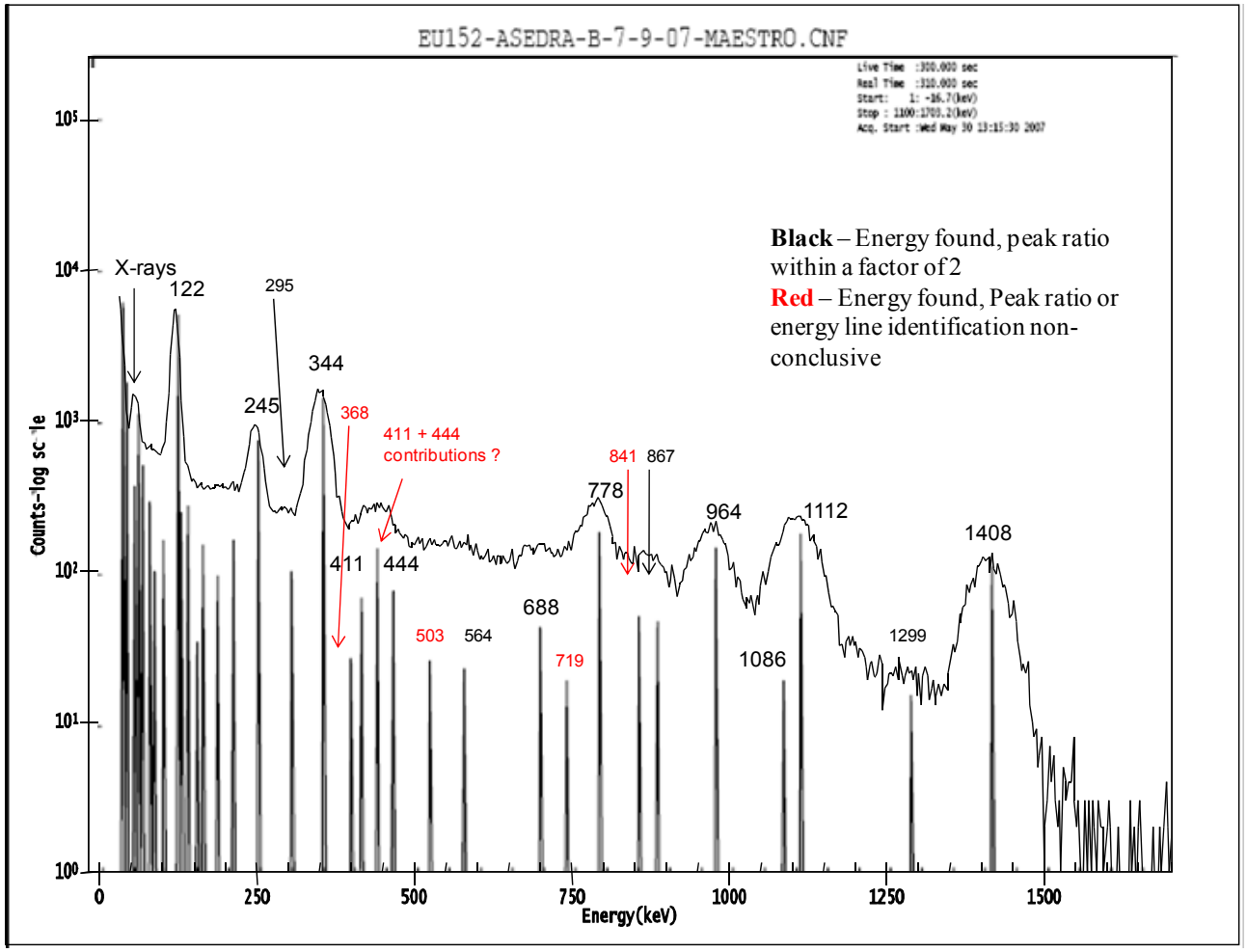

Figure 3.3.1. NaI(Tl) spectrum with photopeak output from ASEDRA, Eu-152, 300 s count

In Figure 3.1.1, the original spectrum is indicated, along with gamma lines separated from the original spectrum as a result of post-processing by ASEDRA shown immediately below the original NaI(Tl) spectrum.

Figure 3.1.1. can be compared directly against a 600 s count using a germanium (HPGe) detector, given in Figure 3.1.2, where known gamma ray lines are indicated.

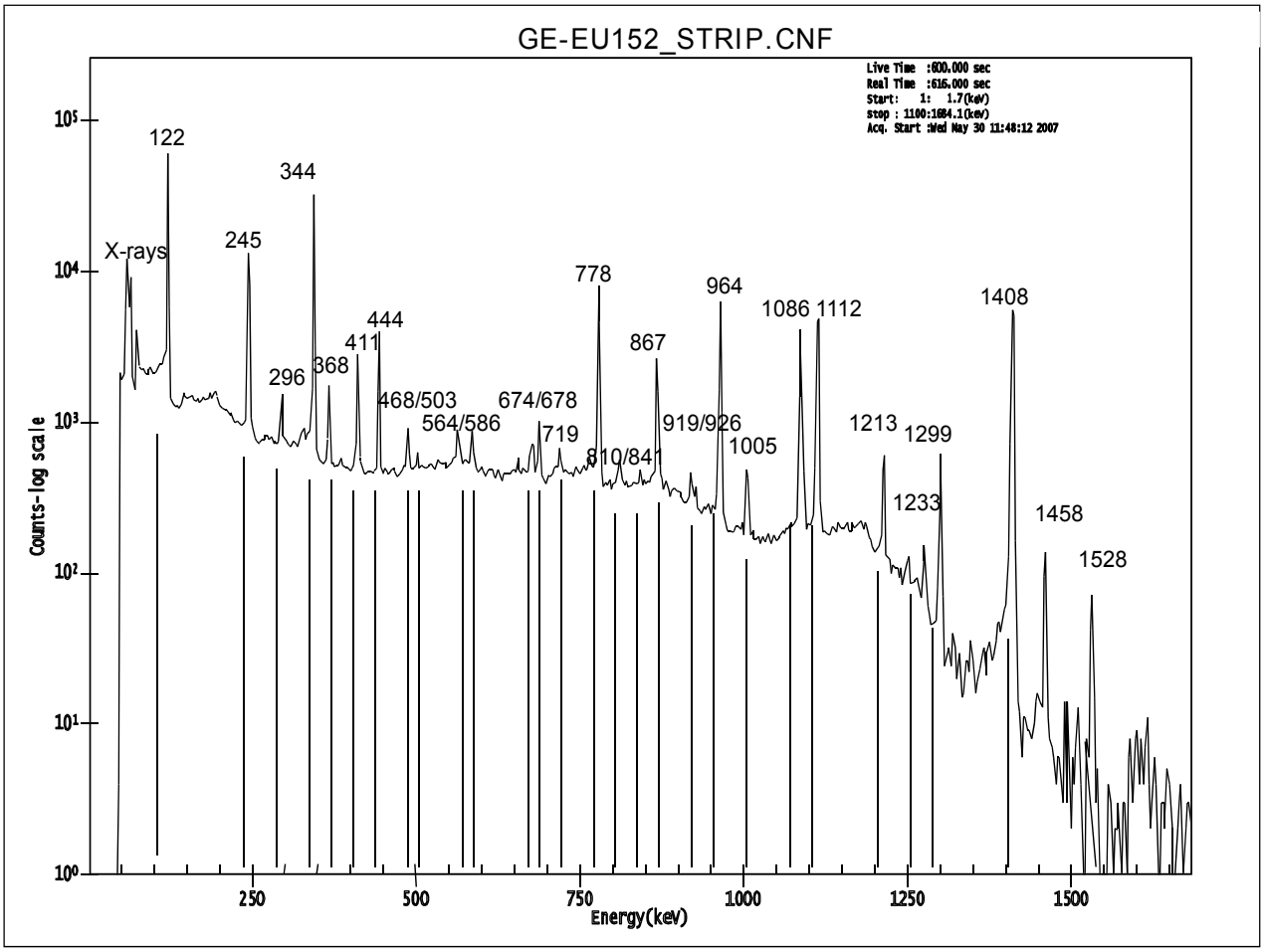

Figure 3.3.2. HPGe reference spectrum with identical source-detector geometry, Eu-152 source, 600 s count

Comparing both Figures 3.1.1 and 3.1.2, one can directly note that a large number of the overlapping energy lines of the ^{152}Eu in the NaI(Tl) spectrum within the energy range of 50 keV to 1500 keV were correctly extracted and identified using ASEDRA.

3.2 Eu-152 Analysis

From inspection of the results, it is readily apparent that ASEDRA does identify all prominent ^{152}Eu lines, as well as several of the weaker lines. Moreover, the ASEDRA identification results (Fig 3.1.1) show peaks which would be particularly difficult to identify with standard peak-fitting routines. One example is identification of the two prominent x-ray peaks, as well as the 1086 keV peak, which is within a detector FWHM of the 1112 keV peak. In addition, of the several lines inconclusively identified between 122 keV and 244 keV in the ASEDRA results, two of these were also identified in the HPGe results, as were the 75, 84, and 96 keV lines. Of note are the 429 keV peak (which may include contributions from the 411 and 444 peaks), as well as a weak 416 keV peak, as well as other weak peaks including the 503 keV and 719 keV peaks, for which the overall yield is close to the ASEDRA peak area cut-off.

In Table 3.2.1, we present the ^{152}Eu energy and Peak yields found, as well as the relative peak ratios for the ^{152}Eu side by side testing of ASEDRA processed NaI(Tl) spectrum with the 600 s HPGe derived spectrum. It is clear that the measured relative ratios shown in Table 3.2.1 are within a factor of 1.5 to 2.0 of the predicted ratios for all but the weakest identified lines in the ASEDRA (NaI) results. The HPGe ratios, in general, are closer to 1.0, as would be expected, since the broader sodium iodide energy resolution and large number of overlapping peaks in the NaI(Tl) spectra collected in 300 s make identifying and fitting all peaks with high accuracy a challenging task.

Table 3.2.1. Results from the ^{152}Eu Analysis: Energy and Yield of Peaks Found and Relative Peak Ratios

Eu-152 Energy, KeV	HPGe Area, (Cts/600 s)	HPGe Ratio to 122 keV	NaI-ASEDRA Energy, keV	NaI (ASEDRA) Area (Cts/300 s)	ASEDRA Ratio to 122 keV (Measured/Predicted)	ASEDRA Ratio to 122 keV (Measured/Predicted)
40.0	4942.0		39.2	6228.1		
45.0	8443.0		45.0	1846.0		
			56.7	383.0		
			62.6	1140.0		
			68.4	525.0		
(75 keV)	13657.0		78.7	303.0		
(84 keV)	9298.0		86.0	106.0		
(96 keV)	8315.0		99.1	168.0		
121.8	102410.0	1.00	121.1	5152.1	1.00	1.73
			125.6	258.0	(125.69 keV)	
			136.2	283.6		
(147 keV)	358.0		149.8	36.2	(148.01 keV)	
			158.9	157.4	(173 keV?)	
(186 keV)	36.0		181.6	98.5	(175 keV?)	
			205.9	169.4	(207.06 keV)	
244.7	20741.0	0.91	243.8	761.8	0.80	1.42
295.9	888.0	0.53	295.4	105.6	1.57	2.80
344.3	71251.0	1.12	344.0	1447.2	0.57	1.00
367.8	1355.0	0.69	387.7	28.9	0.37	0.66
387.9	106.0	16.10				
411.1	4665.0	0.99	404.8	70.0	0.38	0.68
			429.8	148.2	(416.0 keV)	
444.0	5696.0	1.02	454.7	78.5	0.37	0.65
488.0	541.0	0.52				
503.5	245.0	0.93	512.4	27.9	2.86	5.37
534.2	42.0	0.59				
564.0	750.0	0.69	566.8	24.1	0.60	1.06
586.3	469.0	0.66				
656.0	192.0	0.69				
678.6	337.0	0.54				
688.0	530.0	0.34	686.9	45.7	0.79	1.40
719.0	331.0	0.77	729.5	20.4	1.30	2.31
764.9	98.0	0.38				
778.0	14652.0	0.96	781.6	189.6	0.34	0.61
810.0	347.0	0.70				
841.0	187.0	0.74	844.8	53.6	5.95	10.56
867.4	4722.0	1.06	874.8	49.1	0.31	0.55
919.0	190.0	0.32				
926.0	103.0	0.26				
964.0	14242.0	1.01	968.0	150.8	0.31	0.54
1005.3	649.0	0.78				
1085.9	10511.0	1.18	1076.9	20.6	0.07	0.12
1112.1	11917.0	1.03	1103.8	185.4	0.47	0.84
1212.9	1111.0	0.98				
1299.2	932.0	0.74	1285.5	16.5	0.40	0.71
1408.0	15342.0	1.05	1408.9	12.8	0.24	0.43

The ASEDRA ratios are computed in Table 3.2.1 for both the 122 keV and 344 keV peaks, respectively. From these results, the ratios relative to the 122 keV peak show that ratios of energy lines above this peak to drop off compared to predicted results, while ratios relative to the 344 keV peak show the lower energy peaks as inflated and higher energy peaks appear slightly lower than expected. The slight over or underestimation of the relative peak heights is related to the fact that the detector set up was not accounted for in the DRFs originally generated for ASEDRA.

The larger ratios for the lower energy peaks may be over-estimation of counts due to back-scatter and other Compton scattering effects not accounted for in the detector response function determinations integrated into ASEDRA. It should be noted that this could be mitigated by incorporating the exact shielded detector configuration to be used into the Monte Carlo detector responses determined by ASEDRA, thereby accounting for additional Compton and backscatter effects inherent in the measurement. The scattered counts scale factor was set to unity and therefore not used in this test; this is under evaluation. In any event, the number of peaks found and the ability to distinguish close peaks clearly show through in the ASEDRA results.

3.3 WGPU NaI-ASEDRA and HPGe Studies

A second test of ASEDRA using a 10 minute count with shielded Weapons Grade Plutonium (WGPu) gammas (from an encapsulated PuBe source containing 16g of WGPu) was carried out with careful detector calibration, with results presented in Figure 3.3.1 for a 2"x2" NaI(Tl) detector. A very large number of WGPu peaks were extracted by ASEDRA (Figure 3.3.1, left), validated by a co-located, calibrated germanium (HPGe) detector (Figure 3.3.1, right). ASEDRA post-processing required 28 s on a laptop to yield the photopeaks shown. Initial results clearly show that ASEDRA directly separated numerous plutonium gamma peaks (using no prior information), which correlated extremely well to germanium results, as indicated by labels aliasing gamma lines. Initial analysis of the results revealed ASEDRA correctly separated over 90% of the gamma peaks, even those in the low energy region that are difficult to resolve using HPGe due to the inherent Compton scattering in similar regions of the germanium spectrum. A complete investigation of the performance of ASEDRA in identifying gamma signatures from WGPu is reported in a separate publication, and additional evaluations are ongoing [11].

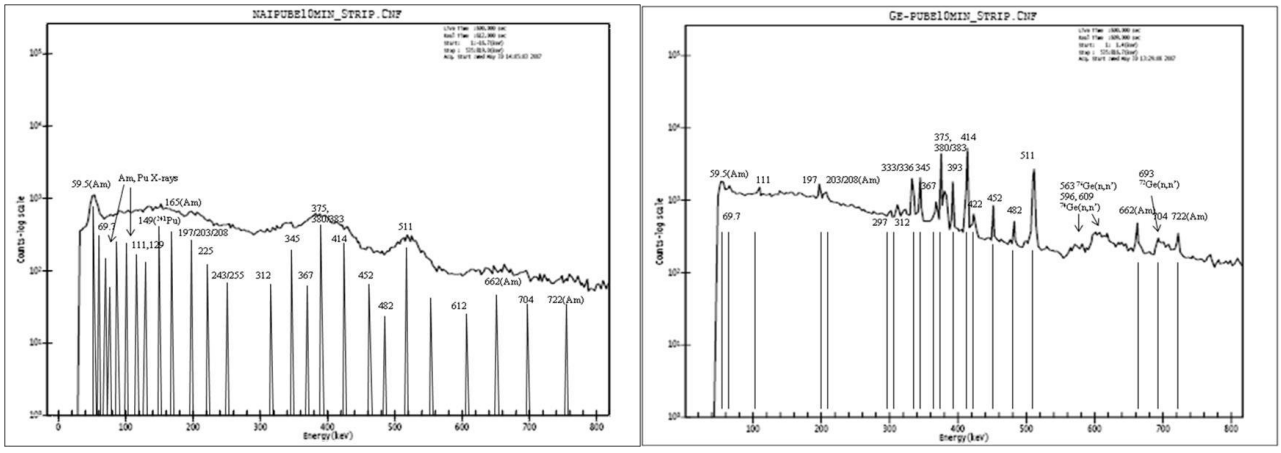

Figure 3.3.1. (Left) NaI(Tl) spectrum output post-processed from ASEDRA, 16 grams of shielded WGPu, 10 min count. (Right). Germanium detector with photopeak output, using the same source and geometry, 10 min count.

4. CONCLUSIONS

In this paper, we present our post-processing algorithm, ASEDRA ("Advanced Synthetically Enhanced Detector Resolution Algorithm"). ASEDRA is designed to post-process scintillator detector spectra to enable photopeaks to be detected with high accuracy, even in the presence of convoluted sources. All current work with ASEDRA has focused on post-processing sodium iodide (NaI(Tl)) scintillator pulse height spectra to synthetically augment the spectrum to enable photopeak identification at a level consistent with detectors operating at approximately one to two percent inherent resolution, depending on the application. Due to the large number of overlapping energy lines in a ^{152}Eu NaI spectra within the energy range of 50 keV to 1500 keV (with over 30 identified in the HPGe spectra), a performance test of ASEDRA with this isotope is a particularly challenging test. Analysis of the ASEDRA results show identification of at least 15 lines from the ^{152}Eu spectra in the ASEDRA output from post-processing, with the relative ratios of yields of the major lines to better than a factor of two, in most cases, relative to ratios with the ^{152}Eu 344 keV peak. Ongoing work with a scattered counts scaling parameter is under investigation to improve relative peak detection characteristics, as are several cases in assessing detection of gammas in WGPu. In any case, testing with ASEDRA reveals that it dramatically augments what is conventionally achievable in sodium iodide scintillators, and is subsequently under commercial development.

REFERENCES

[1] http://www.cbp.gov/xp/cgov/newsroom/fact_sheets/port_security/fact_sheet_cbp_securing.xml
[2] Hofstadter, R., Phys Rev, 74, 100, (1948).
[3] Moszynski, M., "Inorganic scintillation detectors in gamma-ray spectrometry", Nuc. Instr. & Meth. in Phys. Res. A, 505, 101-110 (2003).
[4] Mitchell, D.J., Sodium Iodide Detector Analysis Software (SIDAS). Sandia National Laboratory (1986).
[5] Meng, L., Ramsden, D., IEEE Trans on Nuclear Science, 47-4 (2000).
[6] Likar and Vidmar, Journal of Physics D: Applied Physics, 36, 1903-1909 (2003).
[7] United States Patent and Trademark Office, Provisional Patent 60/971,770, 9/12/2007.
[8] Lavigne, E., Sjoden, G., Baciak, J., and Detwiler, R., "ASEDRA - Advanced Synthetically Enhanced Detector Resolution Algorithm, a Code Package for Post Processing Enhancement of Detector Spectra," FINDS Institute, Nuclear and Radiological Engineering Department, University of Florida (2007).
[9] Lavigne, E., Sjoden, G., Baciak, J., and Detwiler, R., "ACHIP - Adaptive Chi-Square Processing (ACHIP)Code, A package for Noise Reduction of Spectral Response Data," FINDS Institute, Nuclear and Radiological Engineering Department, University of Florida (2007).
[10] Lavigne, E., Sjoden, G., Baciak, J., "A method for stochastic noise reduction by chi-squared analysis," Best of RPSD 2006, Proceedings of the American Nuclear Society 2006 Winter Meeting and Technology Expo, Albuquerque, New Mexico (2006).
[11] Detwiler, R., Sjoden, G., LaVigne, E., and Baciak, J. "Improved plutonium identification and characterization results with NaI(Tl) detector using ASEDRA," SPIE Defense and Security Proceedings #6905-06, Orlando, FL (2008).
[12] X-5 Monte Carlo Team, [MCNP5 - A General Monte Carlo N-Particle Transport Code, Version 5], LA-UR-03-1987, Los Alamos National Laboratory, (2003).